Excitons in the optical absorption spectra of the electroluminescent polymer poly(*para*-phenylenevinylene)

1997 J. Phys.: Condens. Matter 9 5253

(http://iopscience.iop.org/0953-8984/9/24/021)

J. Phys.: Condens. Matter **9** (1997) 5253–5263. Printed in the UK PII: S0953-8984(97)79434-7

Excitons in the optical absorption spectra of the electroluminescent polymer poly(*para*-phenylenevinylene)

Kikuo Harigaya†

Physical Science Division, Electrotechnical Laboratory, Umezono 1-1-4, Tsukuba, Ibaraki 305, Japan

Received 11 November 1996

Abstract. The component of photoexcited states with large spatial extent in the optical absorption spectra of the electroluminescent polymer poly(*para*-phenylenevinylene) (PPV) is investigated by using the intermediate-exciton theory. We find that there is a peak due to long-range excitons on the higher-energy side of the lowest main feature of the optical spectra. The energy position is nearly the same as that of the Hartree–Fock (HF) energy gap. The oscillator strengths of long-range excitons are larger when the electric field of the light is perpendicular to the chain axis. The fact that the onset of the long-range excitons is located near the HF gap might be related to the mechanisms of the large photocurrents measured in this energy region. Next, we calculate the ratio of the oscillator strengths due to long-range excitons to the sum of all of the oscillator strengths of the absorption, as a function of the PPV monomer number. The ratio depends strongly on the system size when the monomer number is low, but the magnitude of the ratio becomes almost constant when the monomer number is more than 10 and near 20, even though slight boundary condition effects persist. Finally, we discuss two different theoretical assignments of the characters of the main features in the absorption of PPV. We show that a large value of the hopping integral is realistic for optical excitations in the neutral PPV chain. The experimental feature at around 5.8 eV is mainly due to localized excitons.

1. Introduction

The observation of remarkable electroluminescent properties of the electroluminescent polymer poly(*para*-phenylenevinylene) (PPV) [1] has attracted physical and chemical research activity. The polymer structure is shown in figure 1. The onset of the photocurrents is located at an excitation energy between 3.0 eV and 4.0 eV [2–4], and this energy is significantly larger than both the optical absorption edge energy at about 2.0 eV and the lowest peak energy at 2.4 eV. This fact has been interpreted theoretically in terms of excitonic effects, which have been taken into account by using the single-excitation configuration-interaction (single-CI) method [5, 6], and also by using the density matrix renormalization group method [7]. The binding energy of the excitons is about 0.9 eV, as has been estimated using the single-CI theory [5].

The spatial extent of the excitons—in other words, the distance between the electrons and holes—might depend on their photoexcitation energies. If an exciton is strongly bound, its extent can be smaller than the region of the PPV monomer unit, and thus the exciton becomes Frenkel-like, as observed in molecular crystals. If the binding is weaker, the photoexcited electron–hole pair tends to distribute over several monomer units, like the charge-transfer

† E-mail address: harigaya@etl.go.jp; URL: http://www.etl.go.jp/People/harigaya/.

0953-8984/97/245253+11$19.50

exciton in molecular systems. The main purpose of this paper is to characterize the extent of the photoexcited states of the PPV by using the single-CI theory recently developed in [6]. Optical excited states with large spatial extent have been pointed out in several earlier papers [8–10]. This paper further characterizes the optical excitations of PPV, bearing in mind the recent measurement of the anisotropy of the spectra with respect to the directions of the electric field of the light [11]. The polymer backbone structure is modelled by means of a tight-binding model Hamiltonian with electron–phonon interactions, and attractions between electrons and holes are taken into account by means of long-range Coulomb interactions. When the distance between an electron and a hole is shorter than the spatial extent of the monomer, we call the exciton a 'short-range' exciton. When the exciton width is larger than the extent of the monomer, we call the exciton a 'long-range' exciton. We shall characterize each photoexcited state as 'short-range' or 'long-range' by calculating the probability that the photoexcited electron and hole exist on different PPV monomer units. A similar characterization method has been used in the recent investigations of charge-transfer excitons in C_{60} cluster systems [12–14], too.

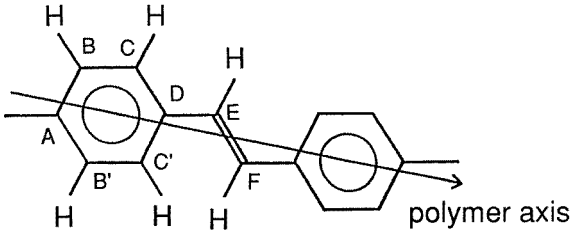

Figure 1. The structure of the PPV chain. The direction of the polymer chain axis is indicated by the arrow. The eight carbon sites, inequivalent to each other, are shown by the labels, A–F, B′, and C′.

We will demonstrate the following properties in this paper.

(1) A long-range exciton feature has its onset at an energy on the higher-energy side of the lowest feature of the optical absorption. The energy position is nearly the same as that of the semiconducting energy gap, which has been interpreted as the onset of the large photocurrents observed in experiments.

(2) The boundary condition effects are apparent when the PPV monomer number is low, but they decrease in strength when the number is about 20.

(3) The sum of the oscillator strengths of the long-range excitons is about 8% of the total oscillator strengths when we use the periodic boundary condition. It becomes about 10% for the open boundary condition. This indicates that boundary condition effects persist in long polymer chains, even if they are weak.

There have been various assignments made of the four peak structures in the optical spectra [5–7]. The third peak in the experiment [3] has been interpreted as being due to the localized exciton in [6], while the fourth peak has been assigned to the localized Frenkel-like exciton in [5, 7]. Both of these assignments are possible, as long as we look at orientationally averaged optical spectra. This inconsistency could be resolved when the anisotropies of the optical spectra with respect to the direction of the electric field of the light are measured. In fact, the recent measurements of the anisotropy favour the assignment of the fourth peak to the localized exciton [11]. Therefore, we conclude that the larger value of the hopping integral is realistic for optical excitations of the neutral PPV chain.

In the next section, the tight-binding model and the calculation method are explained. The calculated results are reported in section 3. The paper is concluded with a summary in section 4.

Table 1. The excitation energies of the four main features. The energy value is not that of the onset of each feature, but is the peak energy. The experimental values are taken from [3], which reports the optical spectra of chemically improved PPV.

Experiment (reference [3])	Theory ($t = 2.0$ eV)	Theory ($t = 2.3$ eV)
2.5 (eV)	2.4 (eV)	2.8 (eV)
3.8	4.2	—
4.7	4.8	4.8
5.8	6.0	5.5
—	—	6.9

2. The model

We consider the following model, with electron–phonon and electron–electron interactions:

$$H = H_{\rm pol} + H_{\rm int} \tag{1}$$

$$H_{\rm pol} = -\sum_{\langle i,j\rangle,\sigma} (t - \alpha y_{i,j})(c^{\dagger}_{i,\sigma} c_{j,\sigma} + \mathrm{HC}) + \frac{K}{2}\sum_{\langle i,j\rangle} y^2_{i,j} \tag{2}$$

$$H_{\rm int} = U\sum_i \left(c^{\dagger}_{i,\uparrow}c_{i,\uparrow} - \frac{n_{\rm el}}{2}\right)\left(c^{\dagger}_{i,\downarrow}c_{i,\downarrow} - \frac{n_{\rm el}}{2}\right) + \sum_{i,j} W(r_{i,j})\left(\sum_{\sigma} c^{\dagger}_{i,\sigma}c_{i,\sigma} - n_{\rm el}\right)\left(\sum_{\tau} c^{\dagger}_{j,\tau}c_{j,\tau} - n_{\rm el}\right). \tag{3}$$

In equation (1), the first term, $H_{\rm pol}$, is the tight-binding model for the PPV polymer backbone (shown in figure 1), with electron–phonon interactions which couple electrons with modulation modes of the bond lengths, and the second term, $H_{\rm int}$, gives the Coulomb interaction potentials among the electrons. In equation (2), t is the hopping integral of the nearest-neighbour carbon atoms in the ideal system without bond alternations; α is the electron–phonon coupling constant that modulates the hopping integral linearly with respect to the bond variable $y_{i,j}$ which measures the magnitude of the bond alternation of the bond $\langle i, j\rangle$; $y_{i,j} > 0$ for longer bonds and $y_{i,j} < 0$ for shorter bonds (the average of $y_{i,j}$ is taken to be zero); K is the harmonic spring constant for $y_{i,j}$; and the sum is taken over the pairs of neighbouring atoms. Equation (3) gives the Coulomb interactions among electrons. Here, $n_{\rm el}$ is the average number of electrons per site; $r_{i,j}$ is the distance between the ith and jth sites; and

$$W(r) = \frac{1}{\sqrt{(1/U)^2 + (r/aV)^2}} \tag{4}$$

is the parametrized Ohno potential used in [6, 12, 14]. The quantity $W(0) = U$ is the strength of the on-site interaction; V means the strength of the long-range part ($W(r) \sim aV/r$ in the limit $r \gg a$); and $a = 1.4$ Å is the mean bond length. We use the long-range interaction, because the excited electron and hole spread over a fairly large region of the system considered. The parameter values used in this paper are $\alpha = 2.59t$ Å^{-1}, $K = 26.6t$ Å^{-2}, $U = 2.5t$, and $V = 1.3t$. They are taken from [6]. Most of the quantities,

in energy units, are given in terms of t in this paper. There are two theoretical types of assignment of the features in the absorption spectra. In the next section, we will compare the theories with experiments by using $t = 2.0$ eV and $t = 2.3$ eV as in table 1.

The excitation wavefunctions of the electron–hole pair are calculated by using the Hartree–Fock approximation followed by the single-CI method. This method has been used on the optical spectra of the PPV chain [5, 6], and C_{60} (C_{70}) molecules and solids [12–15]. The optical absorption spectra become anisotropic with respect to the electric field of the light, as is expected from the polymer structures. Anisotropy effects are considered by applying an electric field in the direction parallel to the chain axis (shown in figure 1), as well as in the perpendicular directions. Usually, two kinds of boundary conditions for the polymer structures are assumed in the calculations. They are periodic and open boundary conditions. The optical spectra may depend on boundary conditions also, so we perform calculations for both cases.

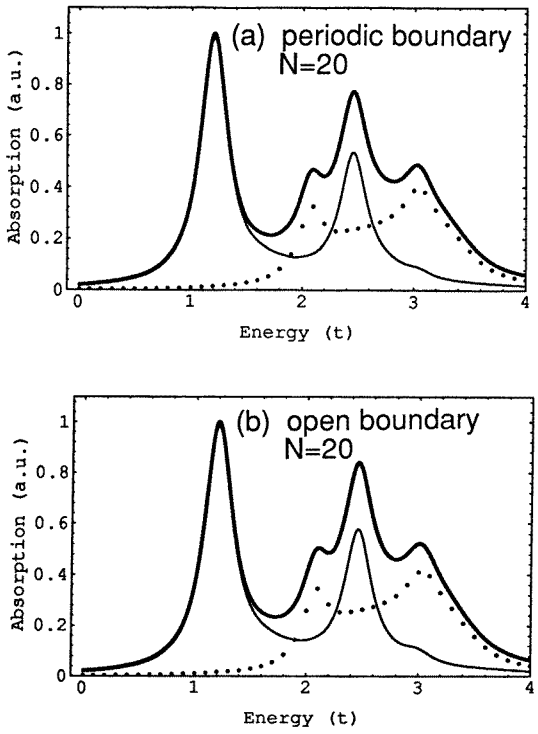

Figure 2. Optical absorption spectra of the PPV for (a) periodic and (b) open boundaries. The number of PPV units is $N = 20$. The bold line is for the total absorption. The thin (dotted) line indicates the absorption where the electric field is along (perpendicular to) the polymer axis. The Lorentzian broadening $\gamma = 0.15t$ is used.

3. Optical absorption spectra of PPV

First, we show the total absorption spectra, and discuss the effects of the boundary conditions and anisotropic effects with respect to the directions of the electric field of the light. Figures 2(a) and 2(b) show the spectra calculated with periodic and open boundaries, respectively.

It seems that the number of PPV monomer units, $N = 20$, determines the spectral shape, almost independently of the chain length. The optical spectra depend strongly on the system size when the number N is less than 10, but they become almost independent of the size when N is near 20. The difference between the spectral shapes for the two boundaries is small also. This is related to the saturated behaviour of the spectral shape.

There are four features, at around $1.2t$, $2.1t$, $2.4t$, and $3.0t$, in the total absorption spectra in figure 2. Anisotropy effects with respect to the electric field are clearly seen: the first and third features are larger when the field is parallel to the polymer axis, while the second and fourth features are larger when the field is perpendicular to the axis.

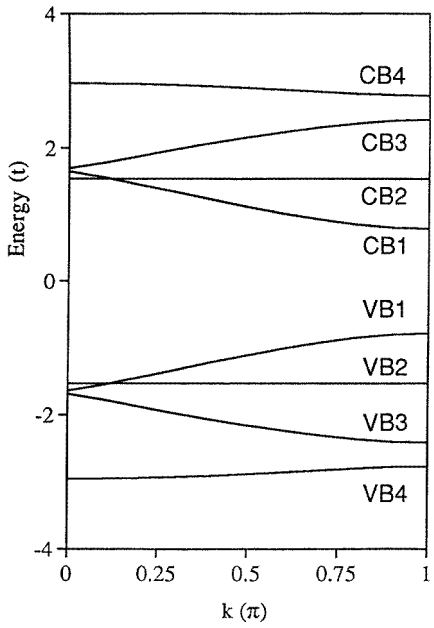

Figure 3. The band structure of the PPV in the Hartree–Fock approximation. There are four branches (named VBj, $j = 1$–4) in the valence band, and there are again four (named CBj, $j = 1$–4) in the conduction band. Just the wavenumber region $0 < k < \pi$ is shown, because of the symmetry. The lattice constant of the unit cell is taken as unity.

In the literature [5–7], two different schemes for the theoretical assignment of the absorption peaks have been proposed. Here, we follow both schemes, by using $t = 2.0$ eV and $t = 2.3$ eV. The results are shown in table 1, compared with the experimental absorption of chemically improved PPV reported in [3]. One scheme [6] is shown in the second column, using $t = 2.0$ eV, and the other [5, 7] is given in the third column, using $t = 2.3$ eV. The degree of agreement between experiments and theories seems comparable for these two schemes, as long as we look at the optical excitation energies. However, the recent measurement of anisotropy [11] favours the assignment with $t = 2.3$ eV: the feature at around 4.7 eV shows anisotropy that is reversed compared to that of the lowest feature, at around 2.5 eV. The assignment of the experiment with $t = 2.3$ eV is consistent with the anisotropy shown in figure 2. Therefore, we find that the larger value of the hopping integral, $t = 2.3$ eV, is realistic for optical excitations of the neutral PPV chain.

Next, we look at the origins of the main features in relation to the band structure. Figure 3 shows the band structure obtained by using the Hartree–Fock approximation. The

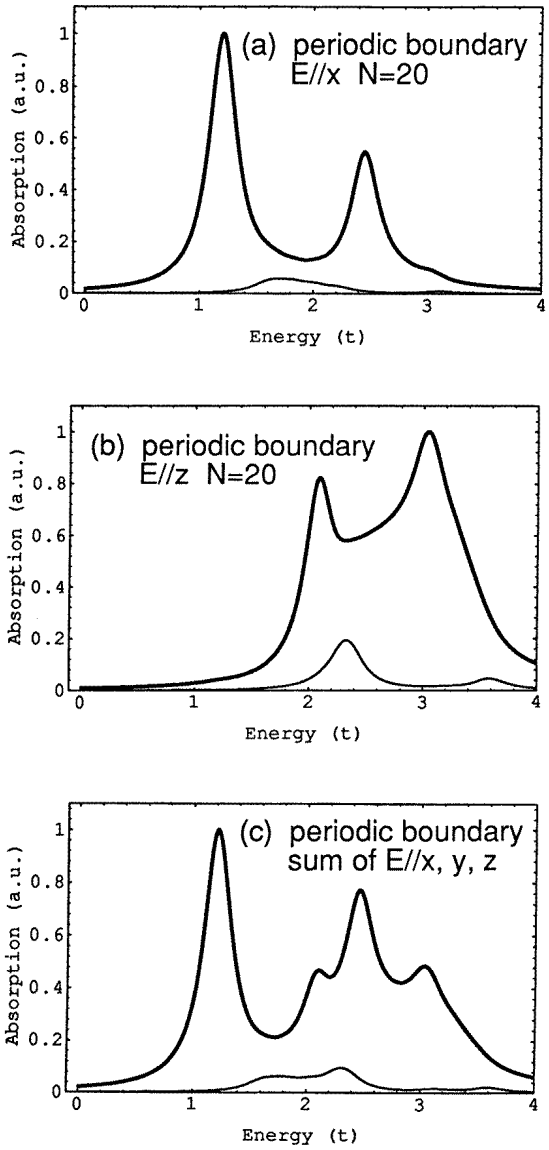

Figure 4. Optical absorption spectra of the PPV with periodic boundaries. The polymer axis is in the x–y plane. The electric field of the light is parallel to the chain and in the direction of the x-axis in (a), and it is perpendicular to the axis and along the z-axis in (b). The orientationally averaged spectra are shown in (c). The number of PPV units is $N = 20$. The bold line is for the total absorption. The thin line indicates the absorption of the long-range component. The Lorentzian broadening $\gamma = 0.15t$ is used.

branches of the valence (conduction) band are named VBj (CBj) (j = 1–4) from the energy gap to band edges. The bands VB2 and CB2 almost lack dispersion. This is due to the fact that the amplitudes at the atoms A and D are nearly zero, and the wavefunctions are localized at the atoms B, C, B′, and C′. Therefore, these two bands are nearly flat. The

experimental feature at around 5.8 eV [3] is mainly due to the optical excitations between these two localized bands. The excitons at around the energy 5.8 eV are nearly localized and Frenkel-like. In the parallel-electric-field case, the dominant first and third features are mainly given by the transitions from VB1 to CB1 bands, and from VB2 to CB2 bands, respectively. In the perpendicular-electric-field case, the large second and fourth features come from transitions from VB1 (VB2) to CB2 (CB1) bands, and from VB2 (VB3) to CB3 (CB2) bands, respectively.

Now, we discuss the long-range component of the optical spectra. The long-range component is defined below. First, we calculate the probability that the photoexcited electron and hole exist on different PPV monomer units. This probability is $1 - 1/N$ for the system with N monomer units, when the electron and hole distribute uniformly. If it is less than $1 - 1/N$, the electron and hole tend to localize in a single monomer unit, and the excited state is like a Frenkel exciton, which is typical for molecular crystals. If the probability is larger than $1 - 1/N$, the electron and hole favour separation into different monomer units, and the excited state has a character like that of a charge-transfer exciton in a molecular crystal. However, the PPV units are connected to each other by real bonds in the polymer, so the term 'charge-transfer exciton' might not be appropriate. Hence, we name such excited states 'long-range' components. We can separate out the contribution to the optical spectra from the long-range component by taking a sum over such states only. We discuss the properties of the long-range component in the following paragraphs.

Figure 4 shows the calculated optical absorption spectra for the periodic boundary case. The bold lines are the total absorption spectra, and the thin lines are the spectra from the long-range component of the excitons. Figures 4(a) and 4(b) show the absorption for the parallel- and perpendicular-electric-field cases, respectively. In figure 4(a), there is a broad peak at around the energy $1.7t$ on the higher-energy side of the feature at $1.2t$. On the higher-energy side of the $2.4t$ feature, the oscillator strengths of the long-range component are very small, and this is consistent with the suggested origin of the $2.4t$ feature: that the bands VB2 and CB2 in figure 3 almost lack dispersion. The optical excitations of this feature tend to localize on a single PPV monomer. In figure 4(b), there are two peaks of the long-range component at around the energies $2.3t$ and $3.6t$, on the higher-energy side of the two main features at $2.1t$ and $3.0t$. Figure 4(c) shows the orientationally averaged spectra. The spectral shape of the long-range component is very broad, and extends from the energy $1.5t$ to about $2.5t$. The threshold of the long-range component is $1.566t$, and this is slightly smaller than the energy of the Hartree–Fock (HF) energy gap, $1.581t$. Therefore, it is very interesting to investigate whether such long-range excitons play a part in the mechanisms of the strong photocurrents which have been measured in the excitation energies between 3.0 eV and 4.0 eV. The oscillator strengths of the long-range component are larger when the electric field is perpendicular to the chain axis.

We calculate the ratio of the sum of the oscillator strengths of the long-range excitons to that of the total absorption—in other words, the ratio of the area below the thin line to the area below the bold line in figure 4. This quantity is calculated for the two electric field directions, and the results are shown as functions of N in figure 5. The ratio depends strongly on the number of monomer units when N is smaller than 10, due to the finite system size. However, the size dependence becomes smaller as N increases. The ratio seems to be almost constant, and the value is about 0.08, near $N = 20$. The ratio is anisotropic with respect to the direction of the electric field of the light. The numerical data for the parallel- and perpendicular-electric-field cases are shown in figure 5, too. We find that the ratio of the perpendicular-field case is slightly larger than that of the parallel-field case. This is related to the fact that the $2.4t$ feature in figure 4(a) has a very small long-range component, and

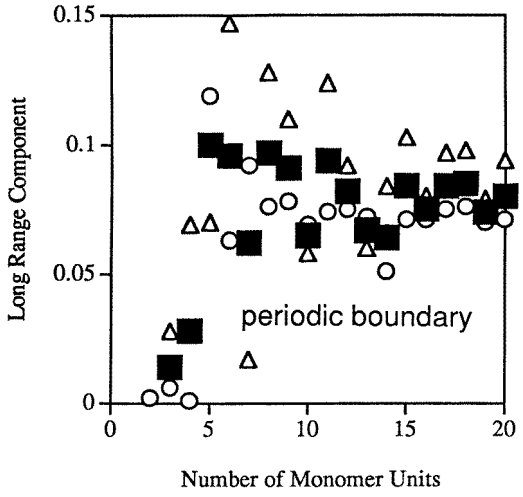

Figure 5. The long-range component of the optical absorption spectra as a function of the PPV unit number N, for the case with a periodic boundary. The squares are for the total absorption. The circles and triangles indicate the data for the cases with the electric field parallel and perpendicular to the polymer axis, respectively.

the electron and hole around this feature tend to localize on a single PPV monomer.

In theories of conducting polymers, calculations have been made for periodic as well as open boundaries. It is of course the case that the boundary effects are small when the system size is relatively large. However, it is of some interest to look at how the boundary effects become smaller as N increases in the present calculations. Figure 6 shows the calculated optical spectra for the open system. The system size has been chosen to be the same as in figure 4, for comparison. The qualitative characters of the long-range components are the same for the two types of boundary conditions. The contribution of the long-range component of the $3.0t$ feature becomes enhanced in figure 6(b) as compared with that of figure 4(b). This is a quantitative difference.

Finally, we calculate the ratio of the oscillator strengths of the long-range excitons to the total contribution, for the open boundary case. The results are shown in figure 7. In the case of the open boundary, the saturation of the ratio as N is increased seems faster than that in figure 5. The value near $N = 20$ is about 0.1, and this is slightly larger than that for the periodic case. A more apparent property is that of the ratio of the perpendicular-electric-field case being much larger than that of the parallel-electric-field case. The anisotropy is larger than that in figure 5. This result is related to the fact that the long-range component of the $3.0t$ feature in figure 6(b) is enhanced as compared with that in figure 4(b). Therefore, we conclude that the qualitative properties of relatively large systems do not depend on the boundary conditions, but quantitative differences remain in the oscillator strengths of the long-range excitons and the anisotropy effects with respect to the electric field.

4. Summary

The spatial extent of photoexcited excitons has been investigated for the optical absorption spectra of PPV. We have found that finite oscillator strengths of long-range excitons exist on the higher-energy side of the lowest main feature of the absorption. The oscillator strengths

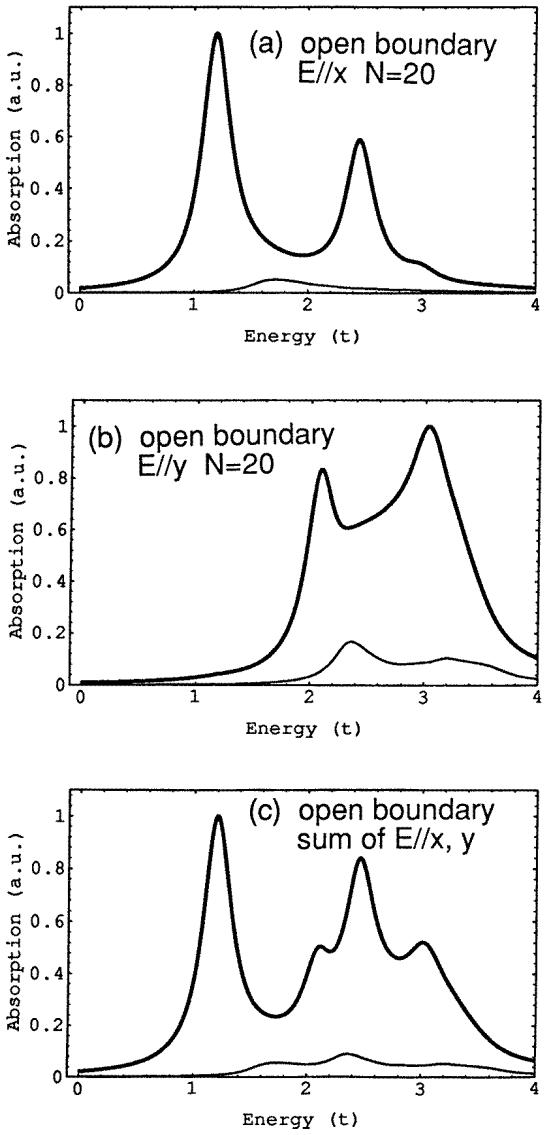

Figure 6. Optical absorption spectra of the PPV with a periodic boundary. The polymer chain is located in the x–y plane. The x-axis is in the direction of the polymer axis, and the y-axis is perpendicular to it. The electric field of the light is parallel (perpendicular) to the chain in (a) (in (b)). The orientationally averaged spectra are shown in (c). The number of PPV units is $N = 20$. The bold line is for the total absorption. The thin line indicates the absorption of the long-range component. The Lorentzian broadening $\gamma = 0.15t$ is used.

of the long-range excitons are larger when the electric field of the light is perpendicular to the chain axis. This indicates an anisotropy due to the polymer structures. The fact that the onset of the long-range excitons, $1.57t$ (=3.60 eV), is located near the HF gap, $1.58t$ (=3.64 eV), might be related to the mechanisms of the large photocurrents measured at around these excitation energies. Next, we looked at the ratio of the total long-range

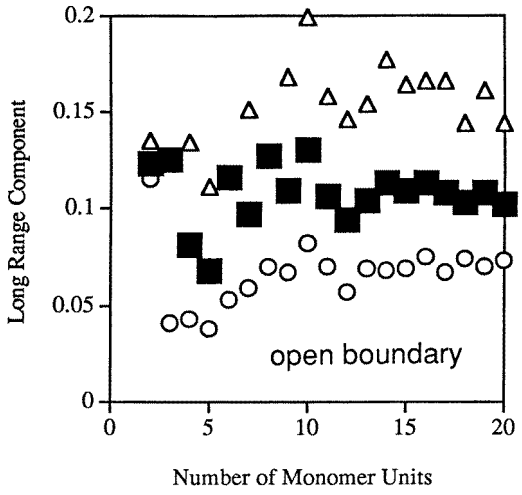

Figure 7. The long-range component of the optical absorption spectra as a function of the PPV unit number N for the case with an open boundary. The squares are for the total absorption. The circles and triangles indicate the data for the cases with the electric field parallel and perpendicular to the polymer axis, respectively.

component to the sum of all of the oscillator strengths, as a function of the PPV monomer number. The ratio depends strongly on the system size when the monomer number is low, but the magnitude of the ratio becomes almost constant when the monomer number is more than 10 and near 20, even though the boundary condition effects remain slight. Finally, we have discussed two different theoretical assignments of the characters of the main features in the absorption of PPV. We conclude that the large value of the hopping integral is realistic for optical excitations in the neutral PPV chain. The feature at around 5.8 eV is mainly due to localized Frenkel-like excitons.

Acknowledgments

Useful discussion with Y Shimoi, S Abe, S Kobayashi, K Murata, and S Kuroda is acknowledged. Helpful communications with S Mazumdar, M Chandross, W Barford, D D C Bradley, R H Friend, E M Conwell, and Z V Vardeny are gratefully acknowledged. Numerical calculations have been performed on the DEC AlphaServer of the Research Information Processing System (RIPS), Agency of Industrial Science and Technology, Japan.

References

[1] Burroughes J H, Bradley D D C, Brown A R, Marks R N, Mackay K, Friend R H, Burn P L and Holmes A B 1990 *Nature* **347** 539
[2] Pichler K, Halliday D A, Bradley D D C, Burn P L, Friend R H and Holmes A B 1993 *J. Phys.: Condens. Matter* **5** 7155
[3] Halliday D A, Burn P L, Friend R H, Bradley D D C, Holmes A B and Kraft A 1993 *Synth. Met.* **55–57** 954
[4] Murata K, Kuroda S, Shimoi Y, Abe S, Noguchi T and Ohnishi T 1996 *J. Phys. Soc. Japan* **65** 3743
[5] Chandross M, Mazumdar S, Jeglinski S, Wei X, Vardeny Z V, Kwock E W and Milter T M 1994 *Phys. Rev.* B **50** 14 702
[6] Shimoi Y and Abe S 1996 *Synth. Met.* **78** 219

[7] Barford W and Bursill R J 1996 *Proc. Int. Conf. on Science and Technology of Synthetic Metals (ICSM96)* (Amsterdam: Elsevier)
[8] Cornil J, Beljonne D, Friend R H and Brédas J L 1994 *Chem. Phys. Lett.* **223** 82
[9] Gartstein Y N, Rice M J and Conwell E M 1995 *Phys. Rev.* B **52** 1683
[10] Mazumdar S and Chandross M 1995 *Proc. SPIE* **2528** 62
[11] Chandross M, Mazumdar S, Liess M, Lane P A, Vardeny Z V, Hamaguchi M and Yoshino K 1997 *Phys. Rev.* B **55** 1486
[12] Harigaya K and Abe S 1994 *Mol. Cryst. Liq. Cryst.* **256** 825
[13] Harigaya K and Abe S 1995 *Proc. 22nd Int. Conf. on the Physics of Semiconductors* (Singapore: World Scientific) p 2101
[14] Harigaya K 1996 *Phys. Rev.* B **54** 12 087
[15] Harigaya K and Abe S 1994 *Phys. Rev.* B **49** 16 746